

# GATSBI: An Online GTSP-Based Algorithm for Targeted Surface Bridge Inspection

Harnaik Dhama, Kevin Yu, Eric Bianchi, Mihil Sreenilayam,  
Kartik Madhira, Matthew Hebdon, and Pratap Tokekar

**Abstract**— We study the problem of visual surface inspecting of a bridge for defects using an Unmanned Aerial Vehicle (UAV). The geometric model of the bridge is unknown beforehand. We equipped the UAV with a 3D LiDAR and RGB camera to build a semantic map of the environment. Our planner, termed *GATSBI*, plans in an online fashion a path to inspect all points on the surface of the bridge. The input to *GATSBI* consists of a 3D occupancy grid map created online with LiDAR scans. Occupied voxels corresponding to the bridge in this grid map are semantically segmented out. Inspecting a bridge voxel requires the UAV to take images from a desired viewing angle and distance. We then create a Generalized Traveling Salesperson Problem (GTSP) instance to cluster candidate viewpoints for inspecting the bridge voxels and use an off-the-shelf GTSP solver to find the optimal path for the given instance. As the algorithm sees more parts of the environment over time, it replans the path. We evaluate the performance of our algorithm through high-fidelity simulations conducted in AirSim. We compare the performance of this algorithm with a frontier exploration algorithm. Our evaluation reveals that targeting the inspection to only the segmented bridge voxels and planning carefully using a GTSP solver leads to more efficient and thorough inspection compared to the baseline algorithm.

## I. INTRODUCTION

Unmanned Aerial Vehicles (UAVs) are increasingly used for visual coverage tasks such as environmental monitoring [1]–[3], surveillance [4], precision agriculture [5], [6], search and rescue [7], [8], and bridge inspection [9]–[16]. We focus on the task of using UAVs for surface inspection of a bridge for defects such as corrosion, rust, fatigue, cracks, etc. that by a human inspector can visually inspect. While UAVs are currently used for bridge inspection, most operations are manual [17]. This requires skillful piloting in high wind conditions. Besides navigational challenges, visual inspection also requires careful planning of viewpoints that obtain high-resolution images covering all points on the surface of the bridge. This is challenging to do manually for a large bridge where one may not always have visual-line-of-sight. To overcome these issues, our group has been developing solutions for assisting manual flights for targeted bridge inspection [18]. We focus in particular on the issue of careful planning of inspection paths for the UAV to ensure

Dhama, Sreenilayam, Madhira, and Tokekar are with the Department of Computer Science & Engineering, University of Maryland, U.S.A. {dhama, msreenil, kmadhira, tokekar}@umd.edu. Yu was with the Department of Electrical & Computer Engineering, Virginia Tech, U.S.A. Email: klyu@vt.edu. Bianchi and Hebdon were with the Department of Civil & Environmental Engineering, Virginia Tech, U.S.A. Email: {beric7, mhebdon}@vt.edu.

This work is supported by the National Science Foundation under grant number 1840044.



Fig. 1: An example of VIEW. The green box represents the face of a bridge voxel, the blue cone represents the viewing cone, and the red band on the cone represents the viewing distance.

high-resolution images of all points on the surface of the bridge.

We say *GATSBI* inspects a point if at some point along the path of the UAV that point falls within the *viewing cone* and *viewing distance* of the camera attached to the UAV (defined in Section III) as illustrated in Figure 1. Our objective is to find a path of minimum length that guarantees inspection of all points on the surface of the bridge.

Inspection is closely related to coverage and exploration, problems that have been well-studied in the literature but, as we will show, are not necessarily the best approaches for inspection. Given a 3D model of the environment, (including the bridge), we can find a coverage path that covers all points on the bridge using an offline planner [19]. In practice, we often do not have any prior model of the layout of the bridges. Even if a prior 3D model is available, it may be inaccurate due to changes in the environment surrounding the bridge as well as structural changes made to the bridge. As a result, we focus on the more general problem of inspecting a bridge without any prior information about its geometry.

Frontier-based strategies [20] are typically used for exploring an initially unknown environment. A frontier is the boundary between explored and unexplored regions. The strategies choose which amongst the set of frontiers to visit (and which path to follow to get to the chosen frontier) to help speed up exploration. The algorithm terminates when there are no more accessible unexplored regions. A bounding

box placed around the bridge can restrict exploration when operating in an open environment. Exploring the bridge does not necessarily mean that the UAV will get inspection quality images. Instead, an inspection planner that can take into account the viewing cone and distance constraints may be more efficient. We present such a planner, termed *GTSP-Based Algorithm for Targeted Surface Bridge Inspection (GATSBI)*, and show that it outperforms the frontier-based exploration strategies efficiently inspecting the bridge (Section V).

GATSBI consists of four modules: 3D occupancy grid mapping using LiDAR data, a semantic segmentation algorithm to find pixels that correspond to the surface of the bridge, a Generalized Traveling Salesperson Problem (GTSP) solver for finding inspection paths for the UAV, and a navigation algorithm for executing the planned path. We use off-the-shelf modules for occupancy grid mapping (Octomap [21]), solving GTSP (GLNS [22]), and point-to-point navigation (MoveIt [23]). Our key algorithmic contribution is to show *how* to reduce the inspection problem to a GTSP instance and the full pipeline that outperforms baseline strategies. Our technique takes into account overlapping viewpoints that can view the same parts of the bridge and simultaneously selects *where* to take images as well as *what order* to visit those locations. We also show when and how to replan as we obtain more information about the environment.

In summary, we make the following contributions:

- present an online algorithm, GATSBI, that plans paths to efficiently inspect bridges when no prior information about them is present;
- evaluate GATSBI (and the effects of parameters within the algorithm) through numerous simulations in AirSim using 3D models of bridges;
- compare GATSBI to a baseline frontier-based exploration algorithm using metrics that capture targeted inspection of bridges.

We organized the paper as follows. In Section II, we review previous work on inspection, coverage, and exploration. In Section III, we present the problem formulation and in Section IV, we describe our solution. In Section V, we present AirSim simulation results. Finally, in Section VI we conclude with a discussion of future work.

## II. RELATED WORK

As described earlier, frontier-based exploration is a widely-used method for 3D exploration of unknown environments [24]–[26]. Others have proposed variants of frontier exploration, in particular, focusing on which amongst the frontiers to choose to visit next [27], [28]. Another popular approach is to model the exploration problem as that of information gathering and choosing a path (or a frontier) that maximizes the information gain [29], [30]. Additionally, there are Next-Best-View approaches [31] that, as the name suggests, plan the next-best location to take an image from in order to explore the environment. We refer the reader to a recent, comprehensive survey on multi-robot exploration by Quattrini-Li [32] that covers a variety of exploration strategies.

As shown in our simulations, generic exploration strategies are inefficient when performing targeted inspection, as in our case. There has been work on designing inspection algorithms that plan paths that take into account the viewpoint considerations [33]–[36]. When prior information is available, one can plan inspection paths carefully by taking into account the geometric model of the environment. Typically, algorithms use prior information, such as a low resolution version of the environment, to create an inspection path and obtain high-resolution measurements of the environment [33], [35]. Unlike these works, we consider a scenario where the robot must plan on incrementally revealed information given no prior environmental information.

Bircher et al. [37] presented a receding horizon planner for both the exploration problem as well as the inspection problem. The two algorithms are similar and use a Rapidly-Exploring Random Tree to generate a set of candidate paths in the known, free space of the environment. Then, they algorithm selects a path based on a criterion that values how much information a path gains about the environment. The planner uses a receding horizon algorithm repeatedly invoked with new information. We follow a similar approach; however, for the work by Bircher et al., the algorithm knows the inspection surface a priori where in our work the only requirement is the UAV sees a portion of the bridge at the start of inspection. The environment is not necessarily known; they test for both known and unknown. GATSBI has no prior knowledge about the environment and minimal knowledge of the target inspection surface.

Song et al. [36] recently proposed an online algorithm which consists of a high-level coverage planner and a low-level inspection planner. The low-level planner takes into account the viewpoint constraints and chooses a local path that gains additional information about the structure under inspection. Our work differentiates by guaranteeing a quality of inspection, not requiring a bounding box around the target infrastructure, and segmenting the infrastructure of interest from the environment which guarantees inspection of only the target infrastructure.

## III. PROBLEM FORMULATION

We describe the overarching problem that we solve as follows.

*Problem 1:* Given a UAV with a 3D LiDAR and RGB camera, find a path to inspect every point on the bridge surface so as to minimize the total flight distance.

We consider the scenario where the geometric model of the bridge is unknown a priori. We assume that the UAV initializes at a location where at least some part of the bridge is visible. If this is not the case, we can run a frontier exploration strategy until such time as when a portion of the bridge is visible.

We then plan an inspection path for the part of the bridge that is visible. As the UAV sees more of the bridge, we replan to find a better tour. Problem 2 (defined shortly) focuses on finding a path for the UAV based on the partial information.

We solve the larger Problem 1 by repeatedly solving Problem 2 as the algorithm gains new information.

We use a 3D semantic, occupancy grid to represent the model of the bridge built online. GATSBI assigns each voxel in the occupancy grid a semantic label. The label indicates whether the voxel is free  $v_F \in V_F$ ; is occupied, part of the bridge, and previously inspected  $v_{BI} \in V_{BI}$ ; is occupied, part of the bridge, but not yet inspected  $v_{BN} \in V_{BN}$ ; and occupied but not a bridge voxel (i.e., obstacles)  $v_O \in V_O$ . The free voxels,  $V_F$ , represent free space where the UAV can fly. The inspected bridge voxels,  $V_{BI}$ , are bridge voxels inspected by the UAV. The non-inspected bridge voxels,  $V_{BN}$ , represent bridge voxels added to the 3D occupancy map, but not yet inspected. Lastly, the obstacle voxels,  $V_O$ , represent occupied voxels that are not the bridge in the 3D occupancy map. Our goal is to inspect all the voxels that correspond to the bridge surface, i.e., to ensure that  $V_{BN} = \emptyset$ .

A voxel  $v_{BN} \in V_{BN}$  is inspected if we inspect at least one of its six faces. A face is inspected if the center of that face falls within a cone given apex angle centered at the UAV camera and within a minimum and maximum range of the UAV camera. The apex angle represents the field-of-view of the camera that is rigidly attached to the UAV. The viewing distance is a minimum and maximum distance range that the UAV should inspect a bridge voxel to ensure quality images for inspection. Figure 1 shows an example of viewing constraints where the green box represents a face of a bridge voxel, the blue cone represents the viewing cone, and the red band on the cone represents the viewing distance. For the rest of the paper, we refer to viewing cone and distance as, VIEW.

*Problem 2:* Given a 3D occupancy map consisting of four sets of voxels ( $V_F, V_{BI}, V_{BN}, V_O$ ), find a minimum length path that inspects every voxel in  $V_{BN}$ .

In the following section we show how to model this problem as a GTSP-instance.

#### IV. THE GATSBI PLANNER

In this section, we give an overview of the GATSBI algorithm. We show the full pipeline Figure 2 which broadly consists of three modules: perception, planning, and execution. We describe each in details next.

##### A. Perception

GATSBI starts by segmenting the bridge from the environment using the LiDAR and RGB sensor information. Each incoming image (Figure 3-left) undergoes semantic segmentation to find pixels corresponding to the bridge.

Using the transformation matrix obtained by extrinsic LiDAR to RGB camera calibration, the algorithm projects the LiDAR data on to the image with a mask. Figure 3-right shows a mask from the color segmentation and Figure 5-row 2 shows masks from the neural network. The 3D points that lie on the segmented bridge classified as bridge points. The point clouds obtained through segmentation using either the colored or neural net segmentors are then fed to

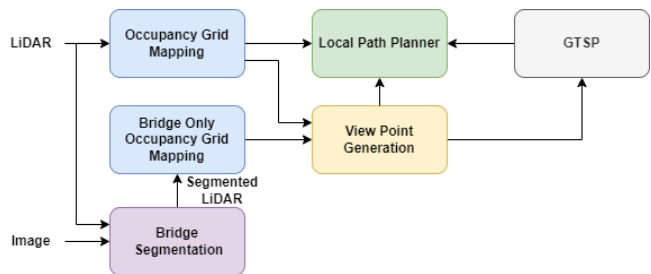


Fig. 2: Flow diagram of GATSBI. The algorithm creates an occupancy grid of the environment using incoming LiDAR scans. Then, it segments the points corresponding to the bridge into another point cloud using the RGB camera images. It then makes another occupancy grid map of only the bridge the segmented point cloud. GATSBI uses both the environment and segmented occupancy maps to generate view points, points in free space where the UAV can inspect the bridge. It sends these to the GTSP instance to make a tour and then a local path planner to get the flight path.

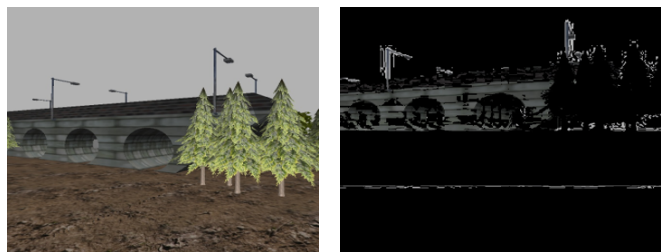


Fig. 3: Left: Single image from the UAV RGB camera. Right: Binary mask created of the image in left.

OctoMap [21] to create a 3D occupancy grid. The output of this module is a set of voxels: free  $V_F$ , bridge  $V_{BI}$ ,  $V_{BN}$ , and obstacle  $V_O$ . The algorithm uses the segmented voxels ( $V_{BI}, V_{BN}$ ) to plan inspection paths. The algorithm uses the other voxels  $V_O$  and  $V_F$  to plan collision-free paths and take into account viewing constraints. We can use either color-based segmentation or neural network-based segmentation of the bridge from the surrounding environment. The neural network-based segmentation method has been previously shown to work robustly with real-world bridge images [38].

##### B. Planner

In order to inspect a bridge, we inspect all voxels in  $V_{BN}$  (as described in Section III). The planner is repeatedly called over time. The  $V_{BI}$  set keeps track of inspected voxels. This avoids unnecessarily inspecting the same voxel more than once (some are unavoidable). Specifically, the UAV must view each voxel in  $V_{BN}$  from some point on its path within VIEW. We formulate this problem as a GTSP instance.

The input to GTSP consists of a weighted graph where the vertices are clusters. The objective is to find a minimum weight tour that visits at least one vertex in each cluster once. GTSP generalizes the Traveling Salesperson Problem and is NP-Hard [22]. In the following, we describe how we

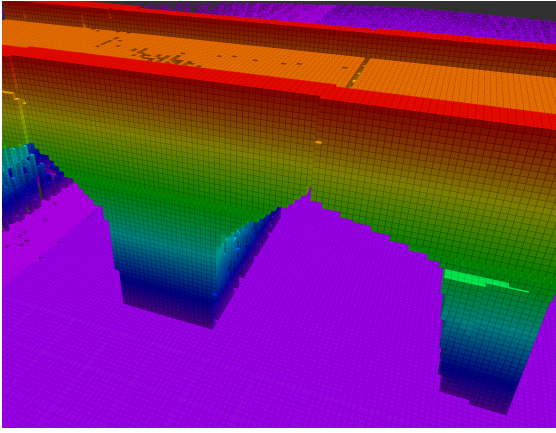


Fig. 4: Full voxel map containing  $V_{BI} \cup V_{BN} \cup V_O$ .

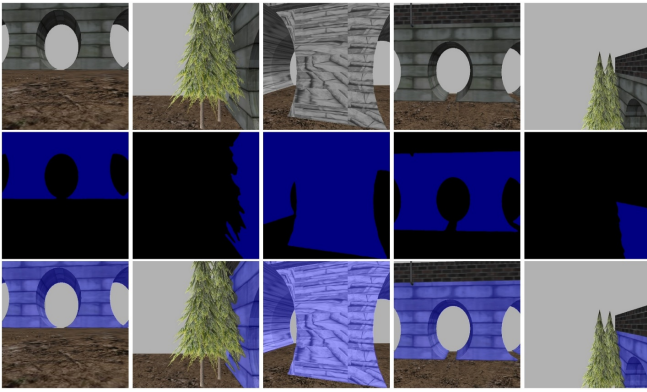


Fig. 5: Example images from neural network. The first row is example images, second row the output mask, and third row is the combined mask and image overlay.

generate the input graph,  $G$ , and clusters for GTSP.

Each vertex in  $G$  corresponds to a candidate viewpoint. We check all pairs of  $v_F \in V_F$  and  $v_{BN} \in V_{BN}$  to see if  $v_F$  lies within VIEW of one of the faces of  $v_{BN}$ . If so, we add a vertex in the graph  $G$  corresponding to the pair  $v_F$  and  $v_{BN}$ . This vertex is also added to the cluster corresponding to each  $v_{BN}$ .

There can be multiple vertices in  $G$  corresponding to the same  $v_F$ , but each such voxel will belong to distinct clusters of  $G$ . If a  $v_F$  does not lie within VIEW of any  $v_{BN} \in V_{BN}$ , then it does not get added to the graph  $G$ .

All free voxels that can inspect the same  $v_{BN}$  will contribute one vertex each to the cluster corresponding to  $v_{BN}$ . The GTSP tour will ensure the UAV visits at least one viewpoint in this cluster.

Next, we create an edge between every pair of vertices in  $G$ . The cost for each of these edges is the Euclidean distance between the two vertices. For vertices in the graph  $G$  that correspond to the same  $v_F$ , the Euclidean distance will equal to zero. With the vertices, edges, and clusters, we create a GTSP instance and use the GTSP solver, GLNS [22], to find a path for the UAV.

### C. Execution

We use the navigation planner software MoveIt [23] to execute the GTSP path. Prior to moving from one point to the next, we check the distance from the current location of the UAV to the next vertex in the GTSP path. We use a point-to-point planner implemented within the MoveIt software based on the work done by Köse [39]. The point-to-point implementation uses an RRT connect solution for finding collision free paths for point-to-point navigation. For the rest of the paper we use the terminology MoveIt to describe using the point-to-point planner. MoveIt [23] finds this distance taking into account the obstacles in the occupancy grid. If the difference between this MoveIt distance and the Euclidean distance is greater than  $DD$  (discrepancy distance), we replan the GTSP path. We replan as needed to ensure that the first edge in the returned tour is within  $DD$  of the MoveIt distance. We call this a lazy evaluation of edge costs. Computing the MoveIt distance (which is a more accurate approximation of the actual travel distances) between every pair of vertices will be time consuming. By checking the discrepancy lazily, we find a tour quickly while also not executing any edge where the actual distance is significantly larger than the expected distance captured by the edge cost.

We keep track of each newly visited cluster during the path flight. Each of these newly visited clusters may correspond to a non-inspected bridge voxel. Once inspected, GATSBI moves them from set  $V_{BN}$  to  $V_{BI}$ . We execute the plan until one of two conditions is met: either a time limit ( $RPT$ ) elapses, or we complete the path, whichever occurs first. We also record the raw sensor data during the flight. The MoveIt planner uses this new data for navigation. Once we complete navigation, we use the stored data to update the bridge inspected and non-inspected voxels and replan. Once  $V_{BN}$  is empty, the GATSBI considers the bridge inspected and terminates.

## V. SIMULATIONS

In this section, we present simulation results to evaluate the performance of GATSBI. We first present a qualitative example of the inspection paths produced by GATSBI. We also evaluate the computational time for 3 subroutines within GATSBI. Finally, we compare GATSBI with the baseline frontier-based exploration.

*Setup:* We use Robot Operating System (ROS) Melodic on Ubuntu 18.04 and both Gazebo and AirSim to carry out the simulations. We equipped the simulated UAV with a LiDAR with specifications set to match a Velodyne VLP-16 3D LiDAR, an RGB camera, and GPS. The 3D LiDAR generates around 300,000 points/sec. It also has a 360° horizontal field of view with  $\pm 15^\circ$  vertical field of view. The VLP-16 has a range of 100m [40]. The localization in simulations is perfect. In the real world, we can use off-the-shelf Visual Inertial Odometry along with GPS for localization along the bridge surface [41], [42].

For all experiments, we use a viewing cone with apex angle of  $0^\circ$  and a viewing distance between 2 to 10 meters. We set the viewing cone to the strictest possibility — a



(a) Steel Bridge



(b) Iron Bridge



(c) Box Girder Bridge



(d) Arch Bridge



(e) Covered Bridge

Fig. 6: The 5 simulation environment bridges.

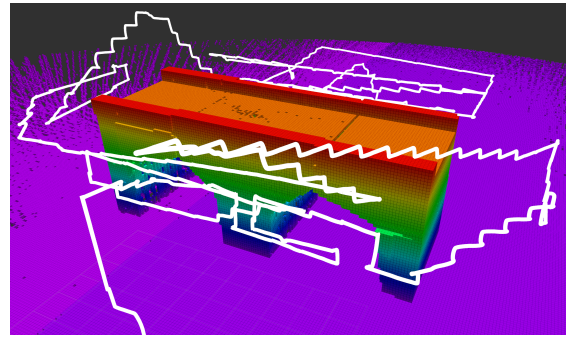


Fig. 7: UAV flight path during GATSBI.

straight line from the camera. This is to ensure the highest quality of images captured for inspection. We set the viewing distance based on [17], where they suggest a minimum flight distance of 2 meters to allow for the safe flight of the UAV.

#### A. Qualitative Example

We evaluate GATSBI on five bridges shown in Figure 6. The five bridges used are the arch bridge, covered bridge, box girder bridge, iron bridge, and steel bridge. All bridges, except the steel bridge, do not contain any other object in the environment except for the ground. The steel bridge, on the other hand, has other distractor objects such as the landscape. They were all chosen because they distinctly represent different types of bridges. Figure 7 shows the path followed by the UAV as given by GATSBI around the Arch Bridge environment.

We also validated the the neural network based segmentation algorithm. We implemented a neural network model from DeeplabV3+ with a ResNet101 backbone [43]. We obtained a total of 439 images from simulation bridges in Gazebo and annotated them using labelme2016 [44]. We split the data into 10% validation and 90% training. The model that we used was fine-tuned from a pre-trained ResNet101 model from PyTorch’s official pre-trained model paths. Training took place using a Tesla V100 GPU. We trained the model for 20 epochs with a validation f1-score of 97.2% and the jaccard-index of 94.7%. This model has also been previously shown to work on real world images. We built the model on images obtained in Gazebo simulations for initial testing. For the rest of the simulation, we use AirSim’s built-in segmentation algorithm. The choice of the segmentation algorithm does not affect the main contribution of this paper, which is the GATSBI planner. Next we present quantitative results on GATSBI.

#### B. Computational Time

We examine the time it takes for executing GATSBI. In Table I, we report the average, minimum, maximum, and standard deviation (std) of the time for all bridges. We report three times: the time spent in the planner to create the GTSP instance (non-GTSP), the time taken to solve the GTSP instance (GTSP), and the flight time before the algorithm calls the planner again (flight). We see that the time it takes GATSBI to perform segmentation and create a

GTSP instance takes a maximum of 0.35 seconds. The GTSP solver takes a maximum of 17.43 seconds. Compared to the flight time (average of approximately 64s), the time taken by the planner is not significant. This suggests that GATSBI is not a bottleneck and is capable of running in real-time on UAVs that are executing 3D bridge inspection in unknown environments.

Bridge	Component	Average	Min.	Max.	STD
Arch	Non-GTSP	0.16s	0.11s	0.24s	0.03s
Arch	GTSP	8.24s	7.50s	9.53s	0.57s
Arch	Flight	58.79s	3.16s	221.52s	38.54s
Covered	Non-GTSP	0.07s	0.03s	0.26s	0.05s
Covered	GTSP	7.56s	7.15s	8.09s	0.26s
Covered	Flight	110.31s	3.55s	417.21s	77.96s
Box Girder	Non-GTSP	0.22s	0.17s	0.29s	0.04s
Box Girder	GTSP	8.78s	7.29s	12.73s	1.18s
Box Girder	Flight	48.41s	0.26s	176.42s	38.47s
Iron	Non-GTSP	0.23s	0.17s	0.30s	0.04s
Iron	GTSP	8.86s	7.29s	11.61s	1.26s
Iron	Flight	50.33s	0.17s	548.56s	55.40s
Steel	Non-GTSP	0.24s	0.15s	0.35s	0.06s
Steel	GTSP	10.65s	7.09s	17.43s	2.83s
Steel	Flight	54.83s	3.84s	185.28s	31.22s

TABLE I: Table showing the time taken for each part of GATSBI over multiple replans.

### C. Comparison with Baseline

We compare the performance of GATSBI with a baseline frontier-based exploration algorithm. Since the baseline method does not directly count the number of inspected voxels, we implement a package on top of the baseline to count the inspected voxels. This way we compare only the inspected voxels not the covered voxels. We can see in Figure 8 that our method does better than the baseline method when comparing the percentage of bridge voxels inspected. We obtain this value by dividing the inspected bridge voxels ( $|V_{BI}|$ ) upon termination of the algorithm by the total inspectable bridge voxels. Note, obstructed bridge voxels that have no candidate viewpoints are uninspectable.

Nevertheless, we observe that GATSBI achieves inspection of 100% voxels while the baseline only achieves a maximum of 10%. Frontier exploration does not explicitly take inspection into account. As shown in the last plot in Figure 8, it performs as well as GATSBI at exploration. The environment is also simple, in a more complicated environment, it would be better at exploration than the GATSBI algorithm. This validates our claim that GATSBI targets inspection of bridge surfaces instead of just covering the environment. We also see that GATSBI executes more thorough inspection than the baseline. Therefore, we justify the claim that GATSBI is more efficient in inspection compared to a frontier exploration algorithm.

## VI. CONCLUSION

We present GATSBI, a method for 3D bridge inspection in an unknown environment. We evaluate the performance of the algorithm through AirSim simulations with a UAV equipped with a 3D LiDAR and an RGB camera. The

simulations show that GATSBI outperforms a frontier-based exploration algorithm. In particular, we show that the algorithm is efficient in the sense that it targets inspectable voxels rather than simply exploring a volume. The simulations also demonstrate that the algorithm can run in real-time. In future work, we intend to spend time on real world experiments.

## REFERENCES

- [1] Peter Liu, Albert Y Chen, Yin-Nan Huang, J Han, J Lai, S Kang, T Wu, M Wen, and M Tsai. A review of rotorcraft unmanned aerial vehicle (uav) developments and applications in civil engineering. *Smart Struct. Syst.*, 13(6):1065–1094, 2014.
- [2] Tolga Ozaslan, Shaojie Shen, Yash Mulgaonkar, Nathan Michael, and Vijay Kumar. Inspection of penstocks and featureless tunnel-like environments using micro uavs. In *International Conference on Field and Service Robotics*, 2013.
- [3] M. Dumbabin and L. Marques. Robots for environmental monitoring: Significant advancements and applications. *IEEE Robotics and Automation Magazine*, 19(1):24–39, Mar 2012.
- [4] Nathan Michael, Ethan Stump, and Kartik Mohta. Persistent surveillance with a team of mavs. In *Intelligent Robots and Systems (IROS), 2011 IEEE/RSJ International Conference on*, pages 2708–2714. IEEE, 2011.
- [5] Jnaneshwar Das, Gareth Cross, Chao Qu, Anurag Makineni, Pratap Tokekar, Yash Mulgaonkar, and Vijay Kumar. Devices, systems, and methods for automated monitoring enabling precision agriculture. In *Proceedings of IEEE Conference on Automation Science and Engineering*, pages 462–469. IEEE, 2015.
- [6] Pratap Tokekar, Joshua Vander Hook, David Mulla, and Volkan Isler. Sensor planning for a symbiotic UAV and UGV system for precision agriculture. *IEEE Transactions on Robotics*, 2016.
- [7] Tristan Sherman, Joshua Tellez, Tristan Cady, Josue Herrera, Hana Haideri, Jimmy Lopez, Mitchell Caudle, Subodh Bhandari, and Daisy Tang. Cooperative search and rescue using autonomous unmanned aerial vehicles. In *2018 AIAA Information Systems-AIAA Infotech@ Aerospace*, page 1490. 2018.
- [8] Yoonchang Sung and Pratap Tokekar. Algorithm for searching and tracking an unknown and varying number of mobile targets using a limited fov sensor. In *Robotics and Automation (ICRA), 2017 IEEE International Conference on*, pages 6246–6252. IEEE, 2017.
- [9] Inkyu Sa and Peter Corke. Vertical infrastructure inspection using a quadcopter and shared autonomy control. In *Field and service robotics*, pages 219–232. Springer, 2014.
- [10] MA Subhan, AS Bhide, and COEB SSGB. Study of unmanned vehicle (robot) for coal mines. *International Journal of Innovative Research in Advanced Engineering (IJIRAE)*, 1(10):116–120, 2014.
- [11] Luke Yoder and Sebastian Scherer. Autonomous exploration for infrastructure modeling with a micro aerial vehicle. In *Field and service robotics*, pages 427–440. Springer, 2016.
- [12] Tolga Özaslan, Giuseppe Loianno, James Keller, Camillo J Taylor, Vijay Kumar, Jennifer M Wozencraft, and Thomas Hood. Autonomous navigation and mapping for inspection of penstocks and tunnels with mavs. *IEEE Robotics and Automation Letters*, 2(3):1740–1747, 2017.
- [13] Kostas Alexis, Georgios Darivianakis, Michael Burri, and Roland Siegwart. Aerial robotic contact-based inspection: planning and control. *Autonomous Robots*, 40(4):631–655, 2016.
- [14] Geoffrey A Hollinger, Urbashi Mitra, and Gaurav S Sukhatme. Active classification: Theory and application to underwater inspection. In *Robotics Research*, pages 95–110. Springer, 2017.
- [15] Najib Metni and Tarek Hamel. A uav for bridge inspection: Visual servoing control law with orientation limits. *Automation in construction*, 17(1):3–10, 2007.
- [16] Je-Keun Oh, Giho Jang, Semin Oh, Jeong Ho Lee, Byung-Ju Yi, Young Shik Moon, Jong Seh Lee, and Youngjin Choi. Bridge inspection robot system with machine vision. *Automation in Construction*, 18(7):929–941, 2009.
- [17] Sattar Dorafshan, Marc Maguire, Nathan V Hoffer, and Calvin Coopmans. Fatigue crack detection using unmanned aerial systems in under-bridge inspection. 2017.
- [18] Prajwal Shanthakumar, Kevin Yu, Mandeep Singh, Jonah Orevillo, Eric Bianchi, Matthew Hebdon, and Pratap Tokekar. View planning and navigation algorithms for autonomous bridge inspection with uavs.

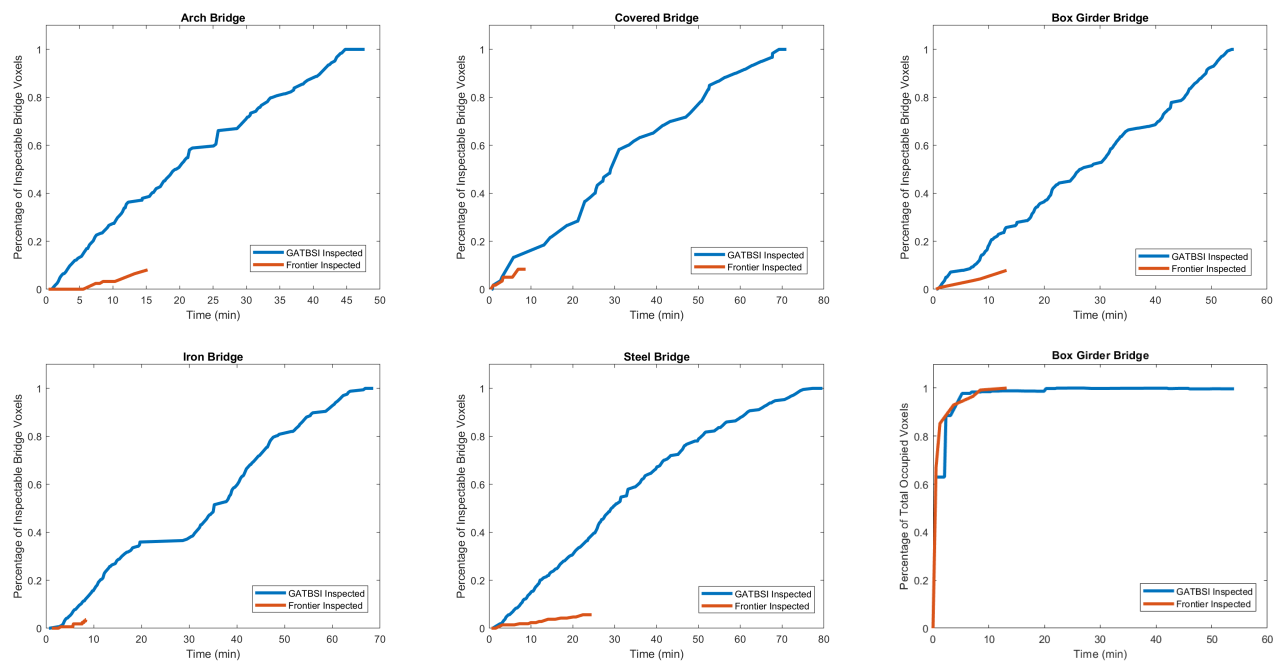


Fig. 8: The GATBSI and Frontier Exploration results. The first 5 figures show the percentage of inspected bridge voxels over time for the 5 bridges. The blue lines are the GATBSI algorithm and the orange is the Frontier Exploration. The last figure shows the number of occupied voxels seen over time in the Box Girder environment.

- In *International Symposium on Experimental Robotics (ISER)*, 2018. Accepted.
- [19] B. Kakillioglu, J. Wang, S. Velipasalar, A. Janani, and E. Koch. 3d sensor-based uav localization for bridge inspection. In *2019 53rd Asilomar Conference on Signals, Systems, and Computers*, pages 1926–1930, 2019.
- [20] Brian Yamauchi. A frontier-based approach for autonomous exploration. In *Proceedings 1997 IEEE International Symposium on Computational Intelligence in Robotics and Automation CIRA'97: Towards New Computational Principles for Robotics and Automation*, pages 146–151. IEEE, 1997.
- [21] Armin Hornung, Kai M. Wurm, Maren Bennewitz, Cyrill Stachniss, and Wolfram Burgard. OctoMap: An efficient probabilistic 3D mapping framework based on octrees. *Autonomous Robots*, 2013. Software available at <http://octomap.github.com>.
- [22] S. L. Smith and F. Imeson. GLNS: An effective large neighborhood search heuristic for the generalized traveling salesman problem. *Computers & Operations Research*, 87:1–19, 2017.
- [23] David Coleman, Ioan Sucan, Sachin Chitta, and Nikolaus Correll. Reducing the barrier to entry of complex robotic software: a moveit! case study. *arXiv preprint arXiv:1404.3785*, 2014.
- [24] Cheng Zhu, Rong Ding, Mengxiang Lin, and Yuanxuan Wu. A 3d frontier-based exploration tool for mavs. In *2015 IEEE 27th International Conference on Tools with Artificial Intelligence (ICTAI)*, pages 348–352. IEEE, 2015.
- [25] Daniel Loubback da Silva Lubanco, Markus Pichler-Scheder, and Thomas Schlechter. A novel frontier-based exploration algorithm for mobile robots. In *2020 6th International Conference on Mechatronics and Robotics Engineering (ICMRE)*, pages 1–5. IEEE, 2020.
- [26] Farzad Nirouei, Ben Sprenger, and Goldie Nejat. Robot exploration in unknown cluttered environments when dealing with uncertainty. In *2017 IEEE International Symposium on Robotics and Intelligent Sensors (IRIS)*, pages 224–229. IEEE, 2017.
- [27] Anna Dai, Sotiris Papatheodorou, Nils Funk, Dimos Tzoumanikas, and Stefan Leutenegger. Fast frontier-based information-driven autonomous exploration with an mav. *arXiv preprint arXiv:2002.04440*, 2020.
- [28] Shaojie Shen, Nathan Michael, and Vijay Kumar. Autonomous indoor 3d exploration with a micro-aerial vehicle. In *2012 IEEE international conference on robotics and automation*, pages 9–15. IEEE, 2012.
- [29] Micah Corah, Cormac O’Meadhra, Kshitij Goel, and Nathan Michael. Communication-efficient planning and mapping for multi-robot exploration in large environments. *IEEE Robotics and Automation Letters*, 4(2):1715–1721, 2019.
- [30] Aravind Preshant Premkumar, Kevin Yu, and Pratap Tokekar. Combining geometric and information-theoretic approaches for multi-robot exploration. *arXiv preprint arXiv:2004.06856*, 2020.
- [31] Richard Pito. A solution to the next best view problem for automated surface acquisition. *IEEE Transactions on pattern analysis and machine intelligence*, 21(10):1016–1030, 1999.
- [32] Alberto Quattrini Li. Exploration and mapping with groups of robots: Recent trends. *Current Robotics Reports*, pages 1–11, 2020.
- [33] Cheng Peng and Volkan Isler. Adaptive view planning for aerial 3d reconstruction. In *2019 International Conference on Robotics and Automation (ICRA)*, pages 2981–2987. IEEE, 2019.
- [34] Geoffrey A Hollinger, Brendan Englot, Franz S Hover, Urbashi Mitra, and Gaurav S Sukhatme. Active planning for underwater inspection and the benefit of adaptivity. *The International Journal of Robotics Research*, 32(1):3–18, 2013.
- [35] Mike Roberts, Debadepta Dey, Anh Truong, Sudipta Sinha, Shital Shah, Ashish Kapoor, Pat Hanrahan, and Neel Joshi. Submodular trajectory optimization for aerial 3d scanning. In *Proceedings of the IEEE International Conference on Computer Vision*, pages 5324–5333, 2017.
- [36] Soohwan Song, Daekyum Kim, and Sungho Jo. Online coverage and inspection planning for 3d modeling. *Autonomous Robots*, pages 1–20, 2020.
- [37] Andreas Bircher, Mina Kamel, Kostas Alexis, Helen Oleynikova, and Roland Siegwart. Receding horizon path planning for 3d exploration and surface inspection. *Autonomous Robots*, 42(2):291–306, 2018.
- [38] Eric Loran Bianchi, Lynn Abbott, Pratap Tokekar, and Matt Hebdon. Coco-bridge: Common objects in context. dataset for structural detail detection of bridges. *ASCE Journal of Computing in Civil Engineering*, 2020. <http://coco-bridge.com>.
- [39] tahsinkose/hector-moveit: Hector quadrotor with moveit! motion planning framework. <https://github.com/tahsinkose/hector-moveit>. (Accessed on 03/03/2021).
- [40] Velodyne puck vlp-16 sensor — lidar — autonomoustuff. <https://autonomoustuff.com/product/velodyne-puck-vlp-16/>. (Accessed on 09/21/2020).
- [41] Burak Kakillioglu, Jiyang Wang, Senem Velipasalar, Alireza Janani, and Edward Koch. 3d sensor-based uav localization for bridge

inspection. In *2019 53rd Asilomar Conference on Signals, Systems, and Computers*, pages 1926–1930. IEEE, 2019.

- [42] Seungwon Song, Sungwook Jung, Hyungjin Kim, and Hyun Myung. A method for mapping and localization of quadrotors for inspection under bridges using camera and 3 d-lidar. In *Proceedings of the 7th Asia-Pacific Workshop on Structural Health Monitoring, Hong Kong SAR, PR China*, 2019.
- [43] Liang-Chieh Chen, Yukun Zhu, George Papandreou, Florian Schroff, and Hartwig Adam. Encoder-decoder with atrous separable convolution for semantic image segmentation. In *Proceedings of the European Conference on Computer Vision (ECCV)*, September 2018.
- [44] Kentaro Wada. labelme: Image Polygonal Annotation with Python. <https://github.com/wkentaro/labelme>, 2016.